JASS Journal of Astronomy and Space Sciences

A Design of Solar Proton Telescope for Next Generation Small Satellite

Jongdae Sohn[1], Suyeon Oh[1], Yu Yi[1†], Kyoung-Wook Min[2], Dae-Young Lee[3], and Jongho Seon[4]

[1]Department of Astronomy and Space Science, Chungnam National University, Daejeon 305-764, Korea
[2]Department of Physics, Korea Advanced Institute of Science and Technology, Daejeon 305-701, Korea
[3]Department of Astronomy and Space Science, Chungbuk National University, Cheongju 361-763, Korea
[4]School of Space Research, Kyung Hee University, Yongin 446-701, Korea

The solar proton telescope (SPT) is considered as one of the scientific instruments to be installed in instruments for the study of space storm (ISSS) which is determined for next generation small satellite-1 (NEXTSat-1). The SPT is the instrument that acquires the information on energetic particles, especially the energy and flux of proton, according to the solar activity in the space radiation environment. We performed the simulation to determine the specification of the SPT using geometry and tracking 4 (GEANT4). The simulation was performed in the range of 0.6-1,000 MeV considering that the proton, which is to be detected, corresponds to the high energy region according to the solar activity in the space radiation environment. By using aluminum as a blocking material and adjusting the energy detection range, we determined total 7 channels (0.6~5, 5~10, 10~20, 20~35, 35~52, 52~72, and >72 MeV) for the energy range of SPT. In the SPT, the proton energy was distinguished using linear energy transfer to compare with or discriminate from relativistic electron for the channels P1-P3 which are the range of less than 20 MeV, and above those channels, the energy was determined on the basis of whether silicon semiconductor detector (SSD) signal can pass or not. To determine the optimal channel, we performed the conceptual design of payload which uses the SSD. The designed SPT will improve the understanding on the capture and decline of solar energetic particles at the radiation belt by measuring the energetic proton.

Keywords: space storm, solar proton, cosmic ray

1. INTRODUCTION

The instruments for the study of space storm (ISSS) is determined for next generation small satellite-1 (NEXTSat-1) to be launched in 2015-2016 and observes the space storm which occurs when the solar activity is in declining phase rather than the solar maximum. The space storm is the fluctuation in near-Earth space caused by an abrupt change of the solar activity such as the solar flare or coronal mass ejection. According to many studies, it is known that the space radiation storm occurs when the solar activity is in declining phase. The ISSS has the purpose of understanding the capture and decline of solar energetic particles at the radiation belt and the ionospheric storm which occurs when there is a geomagnetic substorm.

The Van Allen radiation belt is the region where the energetic particles are trapped by the Earth's magnetic field. It was found in 1958 by Explorer I and II of the United States equipped with the Geiger counter. A lot of studies have been conducted in relation to the radiation belt which is capturing the energetic charged particles. Also, it has continuously been the subject of study in both scientific and engineering aspects such as the way the particles are captured and declined in the radiation belt, the effects of these particles on the space activity such as the spacecraft, and the research related to the satellite operation (Van Allen et al. 1958, Freden 1969, Friedel et al. 2002, Horne et al. 2005, Selesnick et al. 2010). On the other hand, it is known that the cosmic ray flux which is the major source of space radiation decreases as the coronal mass ejection propagates
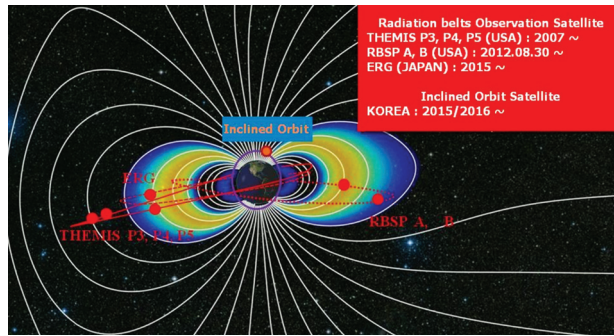
Fig. 1. Satellites observing radiation belt (white line: magnetic field line, inner blue region: inner Van Allen belt, outer blue region: outer Van Allen belt).

Fig. 2. Flux density of particles in the vicinity of the Earth between the Sun and the Earth (Schimmerling & Curtis 1978).

toward the Earth (Oh 2008). This decrease may determine the global phenomena depending on the propagation direction of the coronal mass ejection (Oh et al. 2008, Oh & Yi 2009). And in some cases, the cosmic ray flux observed on the ground increases abruptly, and this is related to the solar energetic particles (Oh et al. 2010). It was found that the increased cosmic ray flux around the Earth is fatally dangerous to the astronauts as well as the spacecraft (Oh et al. 2012). Hence, there is a great need for the study of the solar energetic particles.

The 2015-2016, when the NEXTSat-1 is to be launched, is the time when the solar activity is in declining phase and is optimal for the observation of space storm. As shown in Fig. 1, the time history of events and macroscale interactions during substorms (THEMIS) P3, P4, and P5 satellites operated by the United States since 2007, radiation belt storm probes (RBSP) A and B satellites launched on 30 August 2012, and energization and radiation in geospace (ERG) satellite to be operated by Japan from 2015 all have elliptical orbits on the equatorial plane and are the radiation belt observation satellites which observe or are expected to observe the radiation belt. The NEXTSat-1 is the low earth orbit satellite operated at an altitude of 500-800 km. And it is the sunsynchronous polar orbit satellite which has the noon-midnight orbit. A number of foreign satellites will be operated by the time the NEXTSat-1 is to be launched, and numerous data from the satellites can help to understand the formation and decline of solar energetic particles at the radiation belt.

The solar proton telescope (SPT), which is determined as one of the scientific instruments to be installed in the ISSS, is the instrument that acquires the information on the energy and flux of proton according to the solar activity in the space radiation environment. Especially, the proton from the solar flare is an important source of the particle that we are trying to measure. Fig. 2 compares a lot of
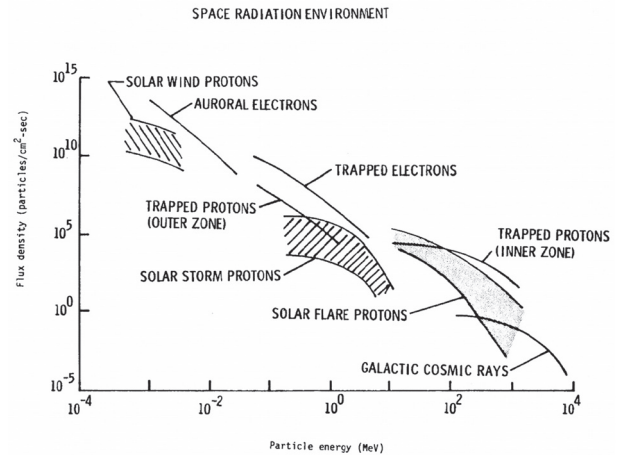
information such as the components and energy band of the particles originating from the space and the Sun, and the particles that are captured in the radiation belt. As shown in Fig. 2, the energy range of the particle is about 10-1,000 MeV and the flux has the range of 1-10^6/(cm²-sec). But there are only few solar energetic protons in the range of 100-1,000 MeV. Therefore, the purpose of the SPT that we design is to measure the solar energetic protons in the range of 0.6-100 MeV. For the channels P1-P3 which are the range of less than 20 MeV, the proton energy was distinguished using linear energy transfer (LET) to compare with or discriminate from relativistic electron, and above those channels, the energy was determined on the basis of whether silicon semiconductor detector (SSD) signal can pass or not.

The payloads such as the medium energy proton and electron detector (MEPED) of polar orbiting environmental satellites (POES), the energetic particle sensor (EPS) of geostationary operational environmental satellite (GOES), and the proton/electron telescope (PET) of Solar, Anomalous, and magnetospheric particle explorer (SAMPEX) are typical high energy particle detectors. They measure the electrons and protons or in some cases, the electrons, protons, and alpha particles. In the case of Korea, the high energy particle detectors installed in existing satellites are the high energy particle telescope (HEPT) of KITSAT-3 and the high energy particle detector (HEPD) of KOMPSAT-1. These equipments were also intended to measure the electrons, protons, and alpha particles. These equipments were successfully loaded to each satellite, but the operation of the equipments was not successful. The SPT that is conceptually designed in this paper is the first proton detector which is determined as the payload of the satellite in Korea. In addition, the components of the

particles captured in the radiation belt are divided into the galactic cosmic ray (GCR) and solar cosmic ray (SCR). The GCR is known to be caused by supernova explosion outside the solar system. The GCR has the energy range of about 100 MeV-10 GeV and the SCR has the energy range of about 10 MeV-1 GeV, which are mostly composed of protons. We will design the detector that measures the solar energetic protons among the particles captured in the radiation belt.

2. SIMULATION USING THE GEANT4

We used geometry and tracking 4 (GEANT4) to determine the specification of the SPT. The GEANT4 was developed in the 1970's, led by European Organization for Nuclear Research (CERN), to simulate the physical activity of the secondary particles generated from large hadron collider (LHC) which is the experimental facility (i.e., particle accelerator and collider) for finding a secret on the formation of the universe by reproducing the big bang which is the situation right after the formation of the universe via colliding two particle beams at nearly the speed of light. In addition, the GEANT4 is the simulation program which tracks the change of state such as the energy, path, and momentum of the incident particle and the change of the path and movement of the secondary particles newly generated through the process according to the interaction between the incident particle and matter based on the physical theory and practical experimental result data, and shows the results as the multi-dimensional image. This program used Fortran language on the basis of Monte-Carlo method, but later it was converted and reconstituted as C++ language which is based on object oriented technology (OOT) (Allison et al. 2006).

In addition to the original purpose, the particle and nuclear physics, the GEANT4 is currently applied to the physical experiments and research activities in various fields such as high energy physics, astrophysics, space science, medical physics, and radiation protection. Especially, it is widely used in the space science field such as the space electronic products, space science detector system, radiation risks simulation for the astronauts, planetary exploration application, linkage to the space environment analysis tool such as SPENVIS, analysis of cosmic ray propagation in the magnetosphere, and micro-dosemetry.

For performing the simulation, we used GEANT4 (9.5.p01 version) and Linux-based operating system. We used the commercial compiler (MS Visual Studio) and Class Library for High Energy Physics (CLHEP, 2.1.2.4 version) with the purpose of physical computation. For the process associated with physical reaction, the standard electromagnetic model which is the most typical mode among the models describing the physical process related to proton was used. The OpenGL graphic driver was used for the visualization which is basically configured in GEANT4. The definitions of the basic physical phenomena included in GEANT4 were appropriately modified according to the simulation planned to be carried out. The standard of experimental space, the standard and position of SPT, and the matter were defined and used. In addition, the SSD was set as the silicon panel, and numerous simulations were performed to obtain an optimal result.

3. METHODS AND RESULTS

The high energy particle incident on a medium loses the energy by the reaction with the medium. In the area that the SPT measures, this LET is the area where it gradually decreases as the energy increases, and given by the Bethe formula (Bethe & Ashkin 1953).

$$-\frac{dE}{dx} = \frac{4\pi}{m_e c^2} \cdot \frac{nz^2}{\beta^2} \cdot \left(\frac{e^2}{4\pi\varepsilon_0}\right)^2 \cdot \left[\ln\left(\frac{2m_e c^2 \beta^2}{I \cdot (1-\beta^2)}\right) - \beta^2\right] \quad (1)$$

where V is the velocity of the particle, C is the speed of light, β is v/c, E is the energy of the particle, x is the travel distance of the particle, z is the charge of the particle, e is the charge of the electron, m_e is the rest mass of the electron, n is the electron density of the target, I is the mean excitation potential of the target, and ε_0 is the vacuum permittivity.

The proton passes through the sensor of the SPT mechanical structure and transfers energy to the bound electrons of silicon by the Coulomb interaction. If the energy loss difference according to the trajectory difference is ignored, the amount of energy in Eq. (1) is approximated by Eq. (2).

$$\Delta\mathbf{E} = \left(-\frac{dE}{dx}\right)t \quad (2)$$

where t is the thickness of the material and ($-dE/dx$) is the LET which is transferred to the material. This energy loss is transformed to an electron-hole pair at the sensor and, by the bias voltage at the sensor, goes to both ends of the silicon sensor where it is converted to an electrical signal.

Table 1 shows the energy channels and channel determination criteria for the SPT, and the SSD signal of each energy channel. We performed the GEANT4 simulation to determine the specification of SPT, and for
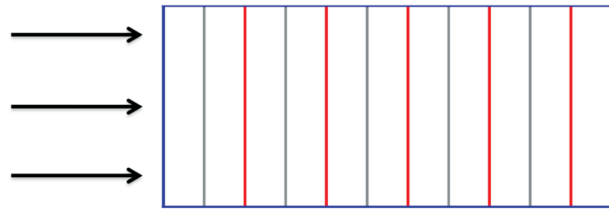
Fig. 3. Arrangement of solar proton telescope on instruments for the study of space storm (red: semiconductor detector, gray: aluminum, blocking material).
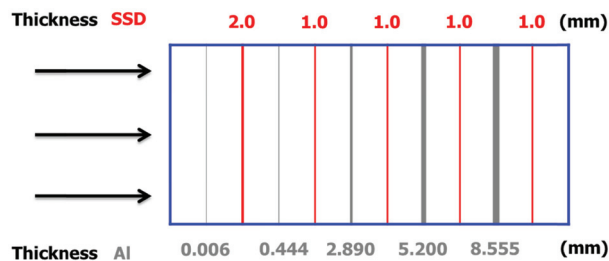

Fig. 4. Structure of solar proton telescope on instruments for the study of space storm (red: semiconductor detector [SSD], gray: aluminum [Al], blocking material).

Table 1. SSD signal of energy channel of SPT on ISSS.

Energy channel (MeV)	SSD1 (MeV)	SSD2	SSD3	SSD4	SSD5
P1	0.6~5.0	0<SSD1<4.9	×	×	×	×
P2	5.0~10.0	4.9<SSD1<9.9	×	×	×	×
P3	10.0~20.0	9.9<SSD1<17.7	×	×	×	×
P4	20.0~35.0	○	○	×	×	×
P5	35.0~52.0	○	○	○	×	×
P6	52.0~71.9	○	○	○	○	×
P7	71.9~	○	○	○	○	○

The symbols (○, ×) represent the detectability (passage) through each SSD of solar energetic protons (○: possible, ×: impossible).
SSD: semiconductor detector, SPT: solar proton telescope, ISSS: instruments for the study of space storm.

Table 2. Structure material and thickness of SPT on ISSS

Material	Thickness (mm)
Al 1	0.006
SSD 1	2.000
Al 2	0.444
SSD 2	1.000
Al 3	2.890
SSD 3	1.000
Al 4	5.200
SSD 4	1.000
Al 5	8.555
SSD 5	1.000

SPT: solar proton telescope, ISSS: instruments for the study of space storm, SSD: semiconductor detector, Al: aluminum.

determining the channel of the detector, the arrangement structure was designed to have the blocking material (aluminum [Al]) and 5 sheets of SSDs as shown in Fig. 3. The SPT detects the electrical signal made by the particle incident at a limited angle due to the mechanical structure of the telescope which passes through the 5 sheets of SSDs (SSD1, SSD2, SSD3, SSD4, and SSD5) arranged in a cylinder type mechanical structure at the back of the telescope and transfers energy to make an electrical signal. Fig. 4 and Table 2 show the structure of the SPT obtained from the simulation results which represent the arrangements of the SSDs and blocking material (Al), and numerical values according to the order that the proton passes through. As shown in Fig. 4, the blocking materials made of Al with the thickness of 0.006, 0.444, 2.890, 5.200, and 8.555 mm are inserted between the 5 sheets of SSDs to distinguish the type and energy of the incident particle. The values in Table 2 were obtained using the brute-force method considering the energy of the incident particle and the energy deposited in the medium.

According to International Commission on Radiation Units and Measurements (1970), the LET of a charged particle in a medium is expressed by dE/dx, and dE is defined as the average energy transferred to the medium by the particle while traveling a distance dx. In the SPT structure, the number of channels was adjusted by placing the blocking material, Al between the SSDs. Here, the average energy transferred to the medium by the particle relative to a travel distance is equivalent to the energy deposited in the medium. In addition, the value for the range of the channel was determined by adjusting the thickness of Al. For the linearly increasing SSD1, the energy will be measured according to the LET by making three channels, and for the rest of the SSDs, the energy will be measured by the flux of the particle collected from the channel for each SSD.

Figs. 5 and 6 are the LET simulation results of energetic proton for the range of 0.6-100 MeV using GEANT4 at the SPT structure in Fig. 4 and Table 1. The values of deposited energy were different depending on the arrangements order and the energy of the incident particle. Also, when the Al1 and Al5 were compared, the values of deposited energy were different depending on the thickness. Fig. 6 shows only the results of the SSDs by eliminating the blocking material, Al from the arrangements of SSD and blocking material in the simulation results of Fig. 5.

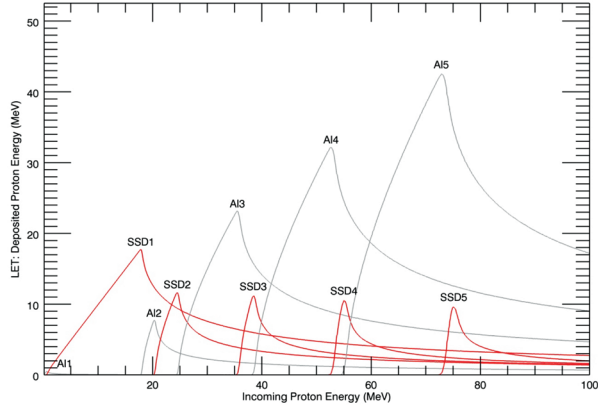If the intensity of the flux incident on SPT is isotropic, the

Fig. 5. Linear energy transfer (LET) simulation of solar proton telescope on instruments for the study of space storm (0.6-100 MeV). SSD: semiconductor detector, Al: aluminum.
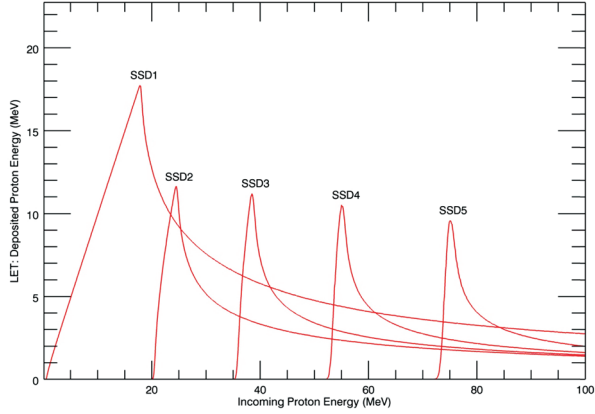

Fig. 6. Linear energy transfer (LET) simulation of solar proton telescope on instruments for the study of space storm (0.6-100 MeV). The blocking materials are omitted from Fig. 5. SSD: semiconductor detector, Al: aluminum.

coincident counting rate (**C**) is expressed by Eq. (3).

$$\mathbf{C} = \mathbf{G} \cdot \mathbf{I} \qquad (3)$$

where **I** is the proton flux and **G** is the geometrical factor which is defined according to the position and width of the detector and detector sensor. The geometric structure of SPT is determined according to **G**, and if the geometric structure of SPT is simplified and assumed to be the symmetrical cylindrical detector as shown in Fig. 2 of Sullivan (1971) which has the two planes of different diameters, the geometrical factor of a typical detector is given by Eq. (4) according to Sullivan (1971).

$$\mathbf{G} = \frac{1}{2}\pi^2 \left[R_1^2 + R_2^2 + H^2 - \left\{ \left(R_1^2 + R_2^2 + H^2 \right)^2 - 4R_1^2 R_2^2 \right\}^{1/2} \right] \qquad (4)$$
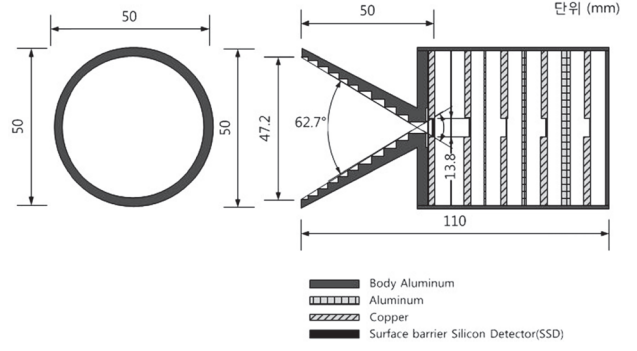

Fig. 7. The expected design structure of solar proton telescope on instruments for the study of space storm.

Table 3. Geometrical factor varying with the distance between collimator and SSD

	distance from front collimator (mm)	Geometrical factor (cm²·sr)
SSD1	50.000	0.846
SSD2	58.344	0.654
SSD3	69.134	0.487
SSD4	82.234	0.355
SSD5	98.689	0.253

SSD: semiconductor detector.

Where R_1 is the radius of collimator aperture, R_2 is the radius of sensor, and H is the distance between R_1 and R_2. The geometrical factor is calculated to be 0.846 cm²·sr when the maximum value of SPT flux is set to 11,825.147/ (cm²·s·sr) which is the maximum flux of the 14 July 2000 event when there was the largest solar proton event during the observation period of PET which is the payload of Solar, Anomalous, and SAMPEX, and the count rate C is assumed to be 10^4/s. The average dead time indicates the time it takes for the detector to process a single signal, and it means that new signals cannot be processed during this time. If the count rate is 10^4/s, the dead time is 10^{-4}s. This time indicates the time which can detect even when the flux is at its minimum. If the flux of solar proton is at the minimum value of 2-3/(cm²·s·sr), the SPT with the geometrical factor of 0.846 cm²·sr is capable of detecting it.

When the T-mount SSD of ORTEC with the same radius of 6.9 mm is used for SPT, the geometrical factor, which is calculated by coincident counting rate, is determined by the radius of collimator aperture, the radius of SSD, and the length interval of collimator. Table 3 shows the values of geometrical factor depending on the distance between the collimator and SSD. Based on the front collimator aperture, the distance is marked according to the arrangement of SSD. The reference position of the collimator is the front part

347

of the collimator which has the diameter of 47.2 mm. The distance from the collimator to the SSD is calculated using the thickness of the T-mount from ORTEC which is 7.9 mm, and the blocking material. The space was not left between the SSD and blocking material to increase the detection efficiency of the detector except for the space occupied by the T-mount and blocking material. The geometric structure of SPT was designed on the basis of the above consideration and it is shown in Fig. 7. It is found that the value of geometrical factor decreases as the distance from the front collimator increases depending on the arrangement of SSD.

4. CONCLUSIONS AND SUMMARY

The ISSS is determined for NEXTSat-1, which is to be launched in 2015-2016, with the purpose of observing the space storm that occurs when the solar activity is in declining phase. It is expected the observation of space storm will help to understand the formation and decline of energetic particles during space storm, and the formation of the radiation belt. The SPT that we are trying to develop is the instrument which acquires the information on the energy and flux of proton according to the solar activity in the space radiation environment. In addition, the proton energy was distinguished using LET for the channels P1-P3, and above those channels, the energy was determined on the basis of whether SSD signal can pass or not. For designing the SPT, a number of calculations and simulations were performed such as the geometrical factor, field of view, and Passage of radiations through matter LET. With the use of GEANT4, we adjusted the energy detection range using the blocking material, Al and determined total 7 channels (0.6~5, 5~10, 10~20, 20~35, 35~52, 52~72, and >72 MeV) for the energy range of SPT. The conceptual design of SPT which uses the SSD was performed and the SPT which has the structure shown in Fig. 7 was designed. The designed SPT will improve the understanding on the capture and decline of solar energetic particles at the radiation belt by measuring the proton.

ACKNOWLEDGMENTS

REFERENCES

Allison J, Amako K, Apostolakis J, Araujo H, Arce Dubois P, et al., Geant4 developments and applications. ITNS, 53, 270-278 (2006). http://dx.doi.org/10.1109/TNS.2006.869826

Bethe H, Ashkin J, Passage of radiations through matter, in Experimental nuclear physics, Vol. 3, ed. Segrè E (Wiley, New York, 1953), 166-357.

Freden SC, Inner-belt Van Allen radiation, SSRv, 9, 198-242 (1969). http://dx.doi.org/10.1007/BF00215633

Friedel RHW, Reeves GD, Obara T, Relativistic electron dynamics in the inner magnetosphere: a review, JAS TP, 64, 265-282 (2002). http://dx.doi.org/10.1016/S1364-6826(01)00088-8

Horne RB, Thorne RM, Shprits Y, Meredith NP, Glauert SA, et al., Wave acceleration of electrons in the Van Allen radiation belts, Natur, 437, 227-230 (2005). http://dx.doi.org/10.1038/nature03939

International Commission on Radiation Units and Measurements (ICRU), Linear energy transfer, ICRU Report Vol. 16 (Oxford University Press, London, 1970), 2-5.

Oh SY, Magnetic cloud and its interplanetary shock sheath as a modulator of the cosmic ray intensity, JASS, 25, 149-156 (2008). http://dx.doi.org/10.5140/JASS.2008.25.2.149

Oh SY, Bieber JW, Clem J, Evenson P, Pyle R, et al., South Pole neutron monitor forecasting of solar proton radiation intensity, SpWea, 10, S05004 (2012). http://dx.doi.org/10.1029/2012SW000795

Oh SY, Yi Y, Statistical reality of globally nonsimultaneous Forbush decrease events, JGR, 114, A11102 (2009). http://dx.doi.org/10.1029/2009JA014190

Oh SY, Yi Y, Bieber JW, Evenson P, Kim YK, Characteristics of solar proton events associated with ground level enhancements, JGR, 115, A10107 (2010). http://dx.doi.org/10.1029/2009JA015171

Oh SY, Yi Y, Kim YH, Globally nonsimultaneous Forbush decrease events and their implications, JGR, 113, A01103 (2008). http://dx.doi.org/10.1029/2007JA012333

Schimmerling W, Curtis SB, Workshop on the radiation environment of the satellite power system (Department of Energy Lawrence Berkeley Laboratory, Berkeley, 1978).

Selesnick RS, Hudson MK, Kress BT, Injection and loss of inner radiation belt protons during solar proton events

and magnetic storms, JGR, 115, A08211 (2010). http://dx.doi.org/10.1029/2010JA015247

Sullivan JD, Geometrical factor and directional response of single and multi-element particle telescope, NucIM, 95, 5-11 (1971). http://dx.doi.org/10.1016/0029-554X(71)90033-4

Van Allen JA, Ludwig GH, Ray EC, Mcllwain CE, Observation of high intensity radiation by satellites 1958 Alpha and Gamma, Jet Propul, 28, 588-592 (1958).